Submitted to

32nd International Conference on High Energy Physics, ICHEP04, August 16, 2004, Beijing

Abstract: **5-0168**

Parallel Session **5**

www-h1.desy.de/h1/www/publications/conf/conf_list.html

Two-Jet and Three-Jet Differential Event Shapes in Deep-Inelastic Scattering

H1 Collaboration

Abstract

Deep-inelastic ep scattering data, taken with the H1 detector at HERA and corresponding to an integrated luminosity of $112\ \mathrm{pb}^{-1}$, are used to study the differential distributions of event shape variables. These include two-jet event shapes (thrust, jet broadening, jet mass and the C-parameter), three-jet event shapes (out-of-event-plane momentum and azimuthal correlation) as well as two, three and four jet rates. The four-momentum transfer Q is taken to be the relevant energy scale and ranges between $14\ \mathrm{GeV}$ and $200\ \mathrm{GeV}$. Fits are performed to the two-jet event shape distributions using next-to-leading order QCD predictions, matched to a leading logarithmic resummation and power law corrections to account for hadronisation effects. The three-jet event shapes and jet rates are compared with QCD calculations and Monte Carlo models.

1 Introduction

Event shapes are designed to study QCD by measuring properties of the flow of hadronic energy-momentum. Measurements of mean values and differential distributions have been carried out at ep [1, 2] as well at e^+e^- [3, 4] colliders. The description of these infrared-collinear safe observables with fixed order calculations faces two difficulties. Firstly, non-perturbative hadronization effects can be large, even at formally perturbative scales. These effects can be addressed with power corrections proportional to $1/Q$[5]. Secondly, the convergence of the perturbative series at low values of the event shape variables is very poor, making a resummation to all orders in α_s necessary.

Results on the analysis of mean values of event shape variables have been published by the H1 Collaboration [2]. These results give support to the concept of power corrections in the approach by Dokshitzer, Webber et al. However, a large spread in the fitted values for α_s lead to the conclusion that higher order QCD corrections are needed.

Resummed NLL calculations, matched to NLO, have recently become available for many of the studied observables[7]. Here, we revisit the topic with a larger data sample and improved data reconstruction and correction techniques. Moreover it is now possible to study the whole spectra instead of only the mean values. Additional event shape variables are investigated, which are sensitive to 3-jet production, and where resummed, matched calculations are near to completion[8]. Therefore in total ten event shape variables are studied. A QCD analysis is presented, based on the five variables for which resummed and matched calculations are available.

2 Event Shape Variables

Hadronic final states in deep-inelastic ep scattering offer excellent possibilities for the study of the predictions of QCD over a wide range of momentum transfer Q in a single experiment. A suitable frame in DIS is the Breit frame, which divides the event into hemispheres corresponding to the proton remnant and the hadronic final state evolving from the struck parton. The definitions of the event shapes treat the hadrons as massless.

Two kinds of 1-thrust, τ and τ_c, the jet broadening B, the jet mass ρ and the C parameter are defined for the particles in the current hemisphere (CH) alone, corresponding to a cut on the pseudorapidity in the Breit frame of $\eta < 0$. The energy in the current hemisphere has to exceed 10% of the total hadronic energy to ensure infrared safety. The definitions of τ and B make explicit use of the virtual boson axis, while the others do not, as is the case for their counterparts in e^+e^- reactions. The exact definitions of these event shapes can be found in [1].

From the point of view of a fixed order calculation, all five of these event shape variables may be labelled “2-jet variables” because, when neglecting hadronization, at least two partons in the final state are needed to obtain non-trivial values. Therefore programs like DISENT and DISASTER++, which calculate 2-jet cross sections to next to leading order in α_s, are suitable for making predictions for this class of event shapes.

In the case of 3-jet event shapes, at least two emissions in addition to the struck quark are needed before these observables can be greater than zero. Examples of 3-jet event shapes for which matched resummed calculations are soon expected are the out-of-event-plane momentum K_{out} and the azimuthal correlation χ. These observables exhibit a rich colour and geometry dependence[8]. The definition of K_{out} is taken from [8], the definition of χ from [9].

The out-of-event plane momentum is defined as

$$K_{\text{out}} = {\sum_h}' |p_h^{\text{out}}| .$$

Here p_h^{out} is the out-of-plane momentum of the hadron h with the event plane formed by the proton momentum $\vec{P}$ in the Breit frame and the unit vector $\vec{n}$ which enters the definition of thrust major:

$$T_M = \max_{\vec{n}} \frac{1}{Q} {\sum_h}' |\vec{p}_h \cdot \vec{n}| , \qquad \vec{n} \cdot \vec{P} = 0 \ .$$

To avoid measurements in the beam region, the sum indicated by ${\sum_h}'$ extends over all hadrons with pseudo-rapidity η in the Breit frame less than 3. The restriction to only the current hemisphere ($\eta < 0$), as for the 2-jet shapes, would be too restrictive in this case, because of the extended phase space available for three partons. For the reasons discussed in [8], only events with $p_t \sim Q$ should be selected, which is accomplished by a cut on the (2+1)-jet resolution y_2 defined by the k_t clustering algorithm: $0.1 < y_2 < 2.5$. Results are presented in terms of K_{out}/Q.

The azimuthal correlation between the hadrons labelled h and i is defined as

$$\chi = \pi - |\phi_h - \phi_i| \ ,$$

where the observable is constructed by summing over all hadron pairs with a weight

$$w = \frac{p_{th} p_{ti}}{Q^2} \ .$$

The azimuth in the Breit frame of hadron h is denoted by ϕ_h. This is the only variable studied which is not a simple differential cross section. In this case a single event contributes not only one value χ to the differential distribution, but instead every pair of hadrons enters with a weight w.

Another class of event shapes, the jet rates, makes use of a jet algorithm. The jet definition used is the k_t clustering algorithm [10]. The jet rate y_n is then defined as the value of the cut parameter y_{cut}, introduced in the jet algorithm, at which the transition from (n +1)-jets to (n)-jets takes place. Since the proton remnant is explicitly treated by the jet algorithm, all hadrons of both hemispheres enter the calculation. Logarithms of the jet rates y_2, y_3 and y_4 are presented here. Up to now no resummed calculations and no power corrections are available. However, jet rates are typically subject to only small hadronization corrections. These corrections have been estimated with the RAPGAP event generator and, in the case of y_2 and y_3, applied on top of a NLO calculation carried out with NLOJET++, to allow for the comparison with the data.

3 Data Sample and Analysis Methods

The analysis is based on an inclusive neutral current DIS data sample. The data cover a large kinematic phase space of $14 \text{ GeV} < Q < 200 \text{ GeV}$ in 4-momentum transfer and $0.1 < y < 0.7$ in the inelasticity y. Seven bins in Q are defined,see table 1. A Bayesian unfolding algorithm[11]

# of Q bin	1	2	3	4	5	6	7
lower bound [GeV]	14	16	20	30	50	70	100
upper bound [GeV]	16	20	30	50	70	100	200

Table 1: Definition of the binning in momemtum transfer Q.

is used to account for detector effects, while QED radiation corrections are applied using HERACLES[6]. This data correction procedure is performed separately for three data samples:

1 $p_P = 820 \text{ GeV}$, $\sqrt{s} \simeq 300 \text{ GeV}$, $\ell = e^+$, $\mathcal{L}_{\text{int}} = 33 \text{ pb}^{-1}$

2 $p_P = 920 \text{ GeV}$, $\sqrt{s} \simeq 318 \text{ GeV}$, $\ell = e^-$, $\mathcal{L}_{\text{int}} = 13 \text{ pb}^{-1}$

3 $p_P = 920 \text{ GeV}$, $\sqrt{s} \simeq 318 \text{ GeV}$, $\ell = e^+$, $\mathcal{L}_{\text{int}} = 66 \text{ pb}^{-1}$

with p_P being the proton beam momentum and ℓ the lepton type. The unfolded distributions from the three samples are all compatible with each other within errors. Sets 1 and 3 are combined by calculating for all bins of the unfolded distributions the luminosity weighted averages.

One is then left with two data sets, one for each lepton charge, which make up the basic result of the experimental measurement. In general, small differences in the event shape distributions between these two data sets are expected, because of weak contributions to the cross section. The different quark coupling of the Z^0 compared to the photon can be thought of as modifying the correlation betweeen the propagator "direction" and the quark directions[16]. Unfortunately, the full calculation of these effects has not yet been carried out. Hence we can only perform QCD fits with calculations for photon exchange. The e^+ and e^- results are thus averaged, appropriately weighted such that part of the Z^0 contribution cancels. The much smaller integrated luminosity of the e^- data enlarges the statistical error of the result due to the cross section weighting. However, for the higher Q-bins, which are statistically limited, this effect is partly cancelled because of the higher inclusive cross section for e^-p scattering. The mean values of Q and x are slightly modified by the combination procedure, giving the final values listed in table 2. The effective centre-of-mass energy of the final combined set is $\sqrt{s} = 316 \text{ GeV}$.

To estimate the experimental systematic error, several studies are carried out. The energy scales of the calorimeters are shifted, the fraction of the recontructed hadronic energy contributed by the tracking devices is varied and two different Monte Carlo models are used for unfolding. In addition, an estimate of an intrinsic bias in the Bayesian unfolding is determined. The errors from the different contributions are added in quadrature.

# of Q bin	1	2	3	4	5	6	7
$\langle Q \rangle$/GeV	14.92	17.74	23.76	36.85	57.58	80.52	115.57
$\langle x \rangle$	0.00841	0.0118	0.0209	0.0491	0.116	0.199	0.323

Table 2: Mean momentum transfer Q and Bjorken x for the seven Q bins of the final distributions.

4 Theoretical Calculations and Fits for 2-jet Variables

A sample of 10^9 DISASTER++ events was generated with the DISPATCH[7] program, making use of the CTEQ5M1[14] parton density functions. The resummation, matched to NLO and the power corrections, is applied with DISRESUM[7]. The matching scheme for each variable is chosen to result in the lowest χ^2 in the fits to the data. Thus for the jet broadening and the C-parameter, ln R matching is utilized, whereas for both versions of thrust and the jet mass, the modified ln R matching is used. For an explanation of the matching see[7].

The distributions depend on two free parameters: $\alpha_s(m_Z)$ the strong coupling constant at the Z^0 mass and $\bar{\alpha}_0(m_I = 2\ \mathrm{GeV})$, the effective coupling of the power correction at an infrared matching scale, chosen to be $2\ \mathrm{GeV}$ by convention. Both parameters are simultaneously fitted for an event shape variable. Bins for which the theoretical calculations are expected to be questionable are omitted from the fit. The definition of χ^2 for the fit takes into account the bin migrations due to limited detector resolution by using a correlation matrix which is calculated by the Bayesian unfolding algorithm. The experimental systematic errors are treated as uncorrelated between the data points.

5 Results

The corrected measured distributions for thrust, jet broadening, the C-parameter and jet mass are shown in figures 1-5, together with the fitted theory prediction. The theoretical predictions are marked with dashed lines for bins which were not included in the fit. A good description of the data by the QCD prediction is evident for the higher values of Q, while for lower Q the distributions are not always well described.

The results for $\bar{\alpha}_0$ and α_s in the form of 1σ contours are given in fig. 6. For comparison a determination of the world average value and error of α_s[12] is shown as a band. A negative correlation coefficient between α_s and α_0 is found for all variables. The universal non-perturbative parameter $\bar{\alpha}_0$ is confirmed to be 0.5 at the 10% level, in agreement with previous analysis in ep scattering[2], which used only the mean values of the event shape variables. In comparison to earlier analyses of mean values in DIS, a smaller spread in α_s is observed. The 1σ contours correspond to the statistical and experimental systematic uncertainties. In addition, the theoretical error is sizeable, mainly due to uncertainty of the renormalization scale. This theoretical error is typically around 5% for both $\bar{\alpha}_0$ and α_s and is therefore at least as large as the experimental error.

Figures 7-9 show the distributions of the 2-jet, 3-jet and 4-jet rate, figures 10 and 11 the distributions of the 3-jet event shapes K_{out} and χ. For the jet rates and the 3-jet event shapes, no fits were performed up to now. Results from NLOJET++ give a good description of y_2 and y_3 for higher values of Q. The jet rate y_4 and the 3-jet event shapes are well described by the RAPGAP Monte Carlo event generator using LO matrix elements with parton showers.

6 Conclusion

It has been shown earlier[2] that power corrections are applicable in the describtion of the non-perturbative hadronization of event shape mean values. With the present analysis we extend the analysis to the whole differential distributions. Theory predictions based on resummed terms matched with fixed order calculations and power corrections, which are presented for thrust, jet broadening, the C-parameter and jet mass, describe the data well. Fits of the free parameters of these calculations, α_s and $\bar{\alpha}_0$ lead to consistent results. The completion of the generalized resummation program, which is currently underway[15], is eagerly awaited for the y_2, y_3, K_{out} and χ variables.

References

[1] C. Adloff *et al.* [H1 Collaboration], Phys. Lett. B **406** (1997) 256 [hep-ex/9706002].

[2] C. Adloff *et al.* [H1 Collaboration], Eur. Phys. J. C **14** (2000) 255. Erratum-ibid. C **18** (2000) 417 [hep-ex/9912052].

[3] P. A. Movilla Fernandez, O. Biebel and S. Bethke, [hep-ex/9906033].

[4] J. Abdallah *et al.* [DELPHI Collaboration], CERN-EP-2002-082.

[5] Y. L. Dokshitzer and B. R. Webber, Phys. Lett. B **404** (1997) 321 [hep-ph/9704298].

[6] A. Kwiatkowski, H. Spiesberger and H. J. Mohring, Comput. Phys. Commun. **69** (1992) 155.

[7] M. Dasgupta and G. P. Salam, JHEP **0208** (2002) 032 [hep-ph/0208073].

[8] A. Banfi, G. Marchesini, G. Smye and G. Zanderighi, JHEP **0111** (2001) 066 [hep-ph/0111157].

[9] A. Banfi, G. Marchesini and G. Smye, JHEP **0204** (2002) 024 [hep-ph/0203150].

[10] S. Catani, Y. L. Dokshitzer and B. R. Webber, Phys. Lett. B **285** (1992) 291.

[11] G. D'Agostini, Nucl. Instrum. Meth. A **362** (1995) 487.

[12] S. Bethke, J. Phys. G **26** (2000) R27 [hep-ex/0004021].

[13] D. Graudenz, [hep-ph/9710244].

[14] H. L. Lai *et al.* [CTEQ Collaboration], Eur. Phys. J. C **12** (2000) 375 [hep-ph/9903282].

[15] A. Banfi, G. P. Salam and G. Zanderighi, hep-ph/0304148.

[16] M. Dasgupta, G. P. Salam, private communication.

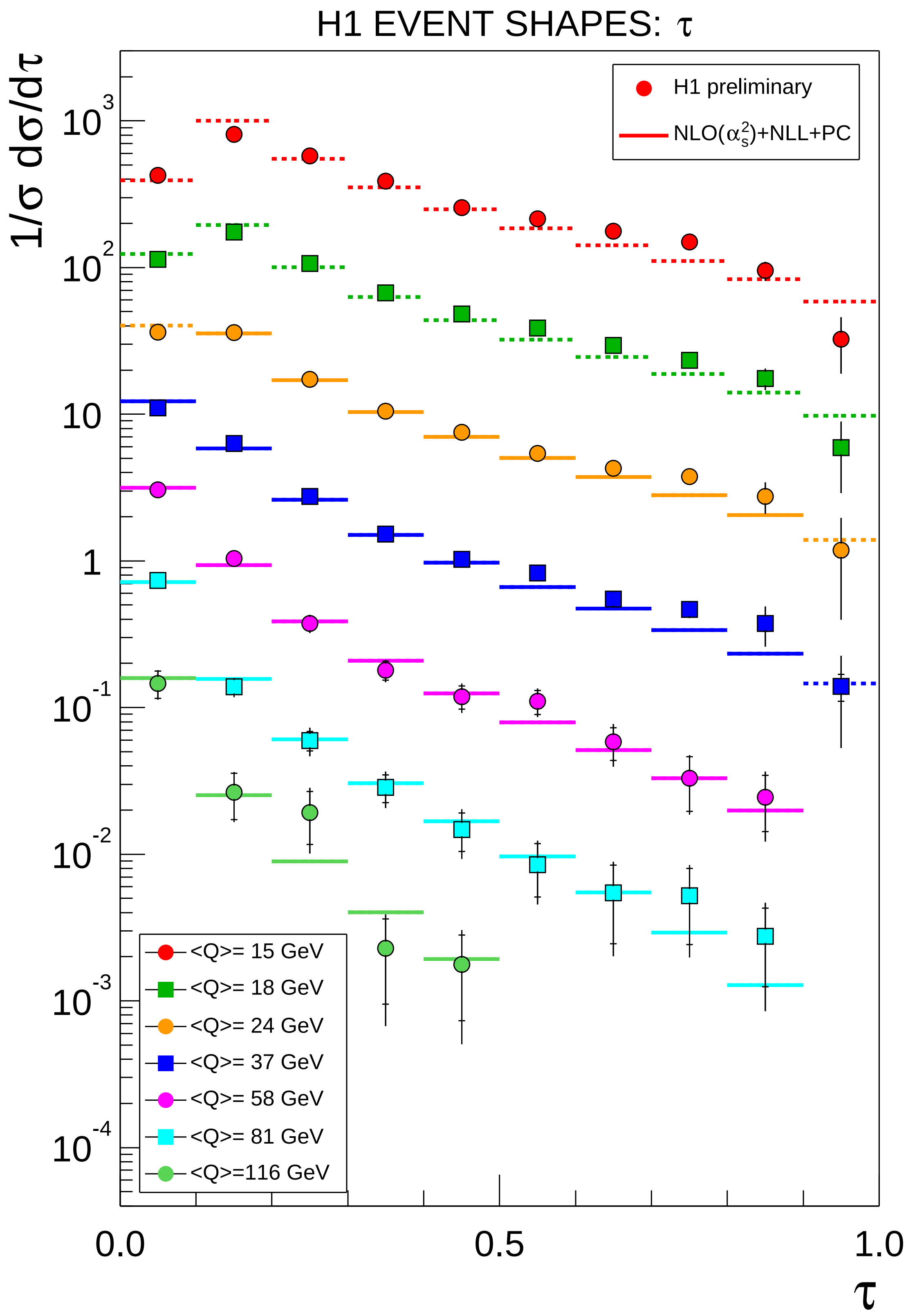

Figure 1: Measured values of $1-$ thrust, τ, averaged over e^+ and e^- data. The data are compared with the results of a fit based on NLO QCD including resummation and power corrections. The fit predictions are shown with dashed lines for those data points which were not included in the fit.

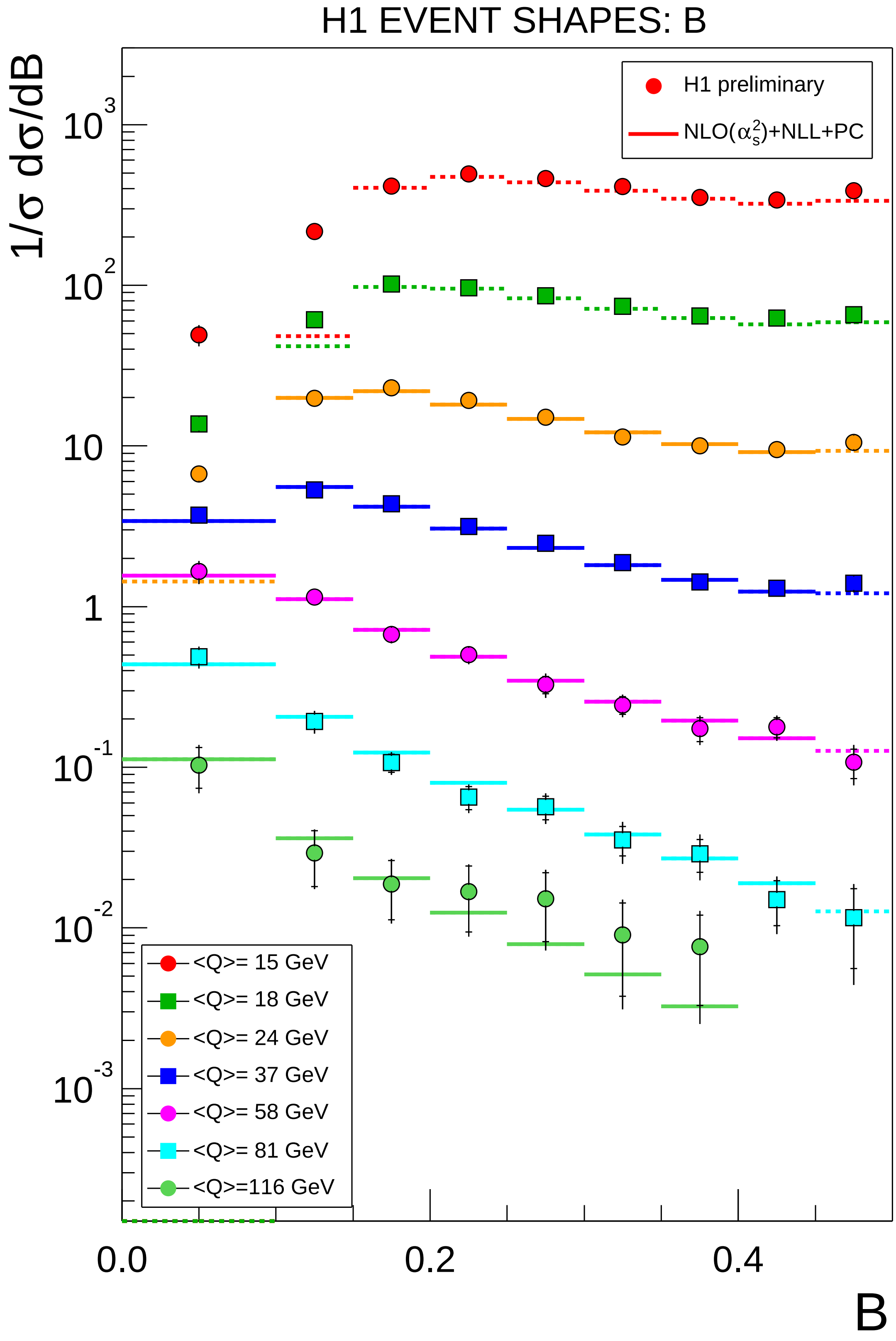

Figure 2: Measured values of jet broadening B, averaged over e^+ and e^- data. The data are compared with the results of a fit based on NLO QCD including resummation and power corrections. The fit predictions are shown with dashed lines for those data points which were not included in the fit.

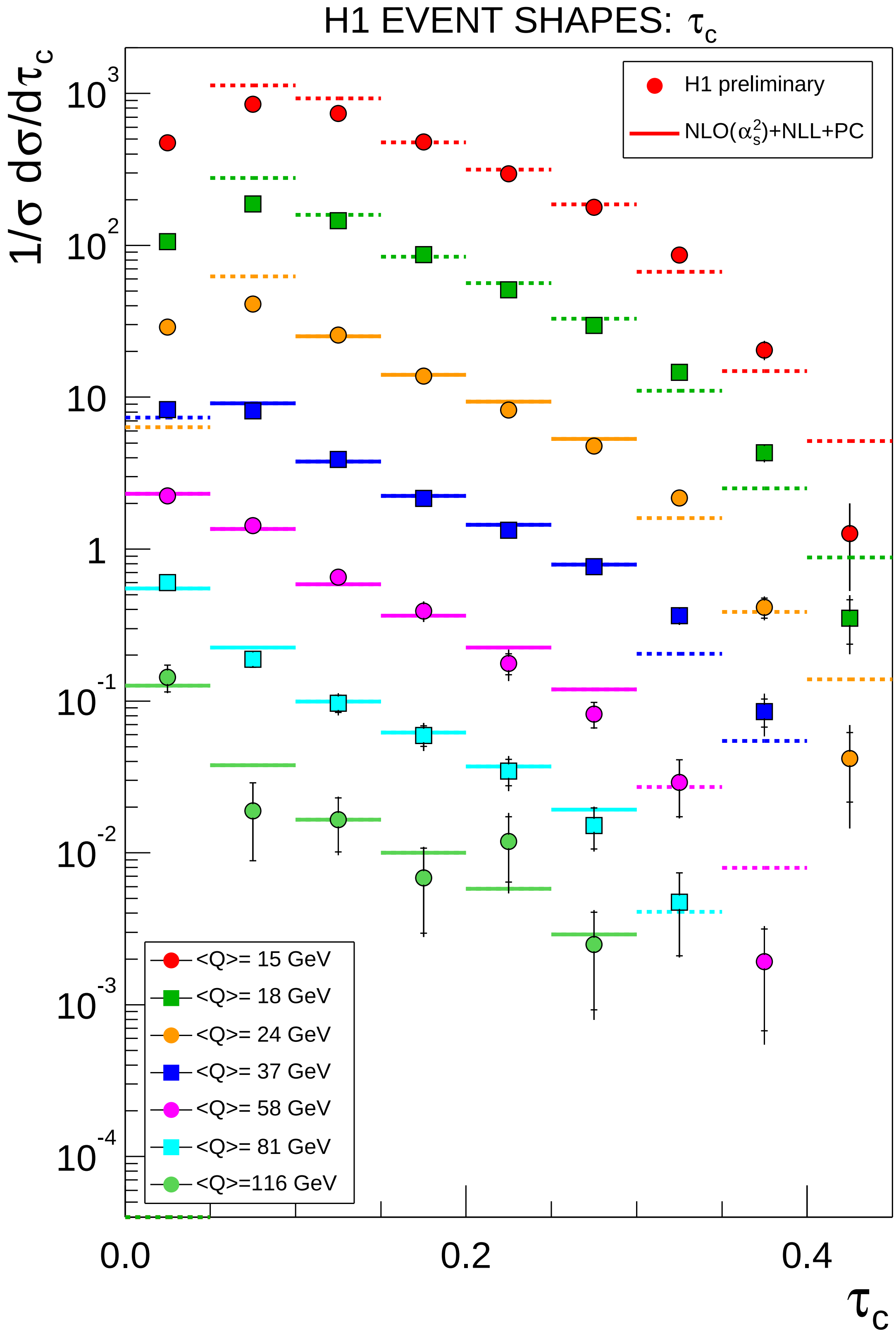

Figure 3: Measured values of $1-$ thrust, τ_c, averaged over e^+ and e^- data. The data are compared with the results of a fit based on NLO QCD including resummation and power corrections. The fit predictions are shown with dashed lines for those data points which were not included in the fit.

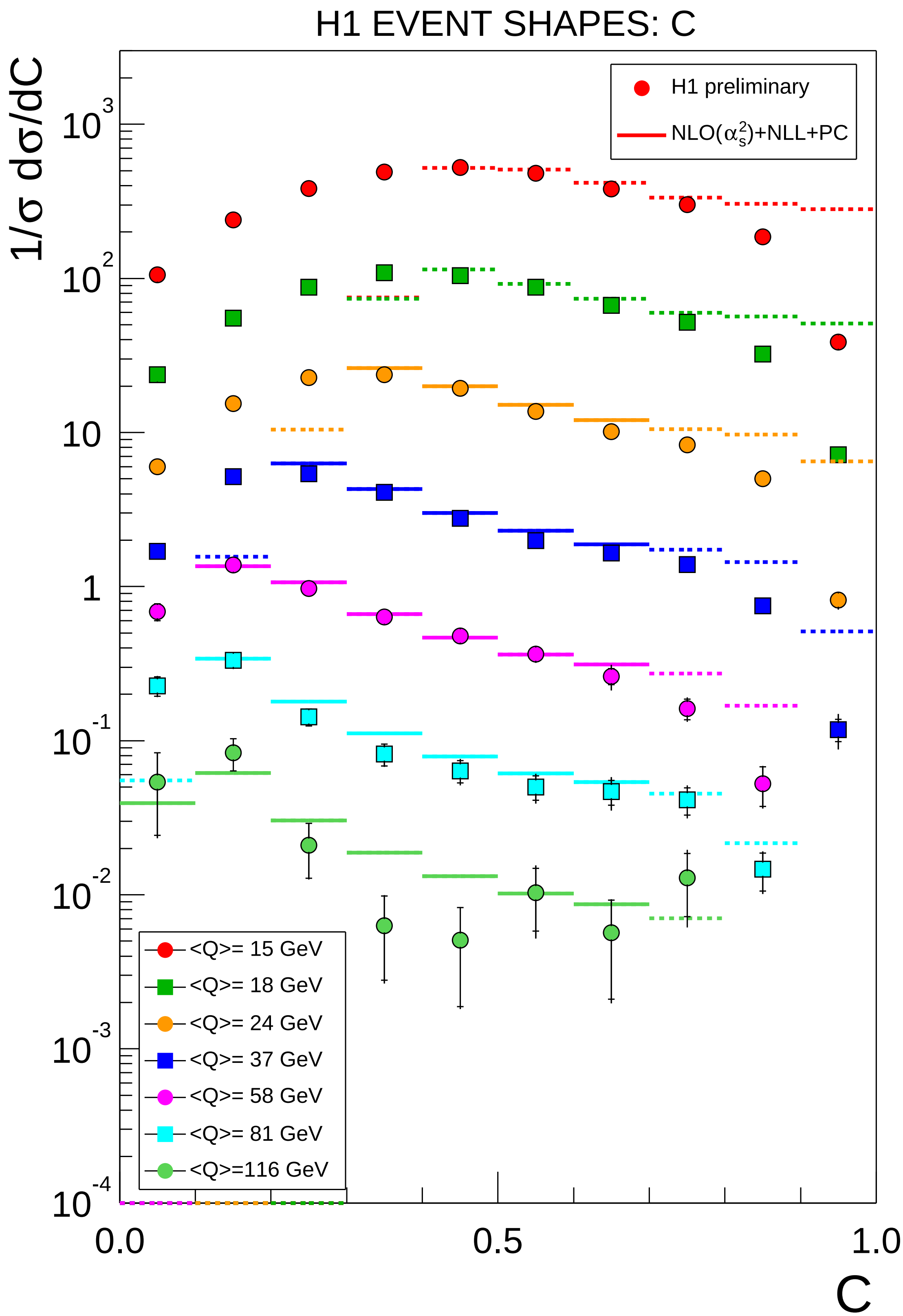

Figure 4: Measured values of the C-parameter, averaged over e^+ and e^- data. The data are compared with the results of a fit based on NLO QCD including resummation and power corrections. The fit predictions are shown with dashed lines for those data points which were not included in the fit.

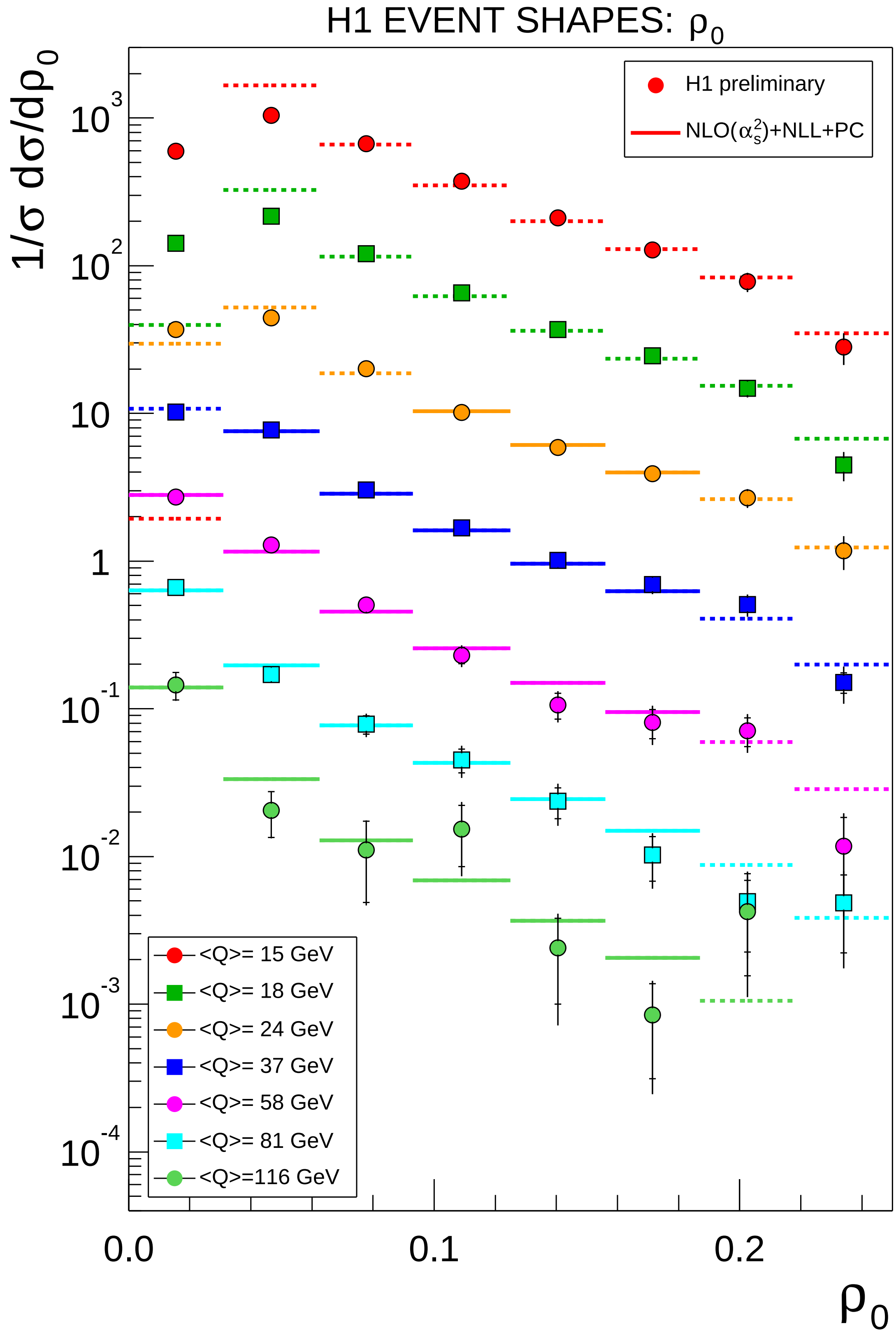

Figure 5: Measured values of jet mass ρ_0, averaged over e^+ and e^- data. The data are compared with the results of a fit based on NLO QCD including resummation and power corrections. The fit predictions are shown with dashed lines for those data points which were not included in the fit.

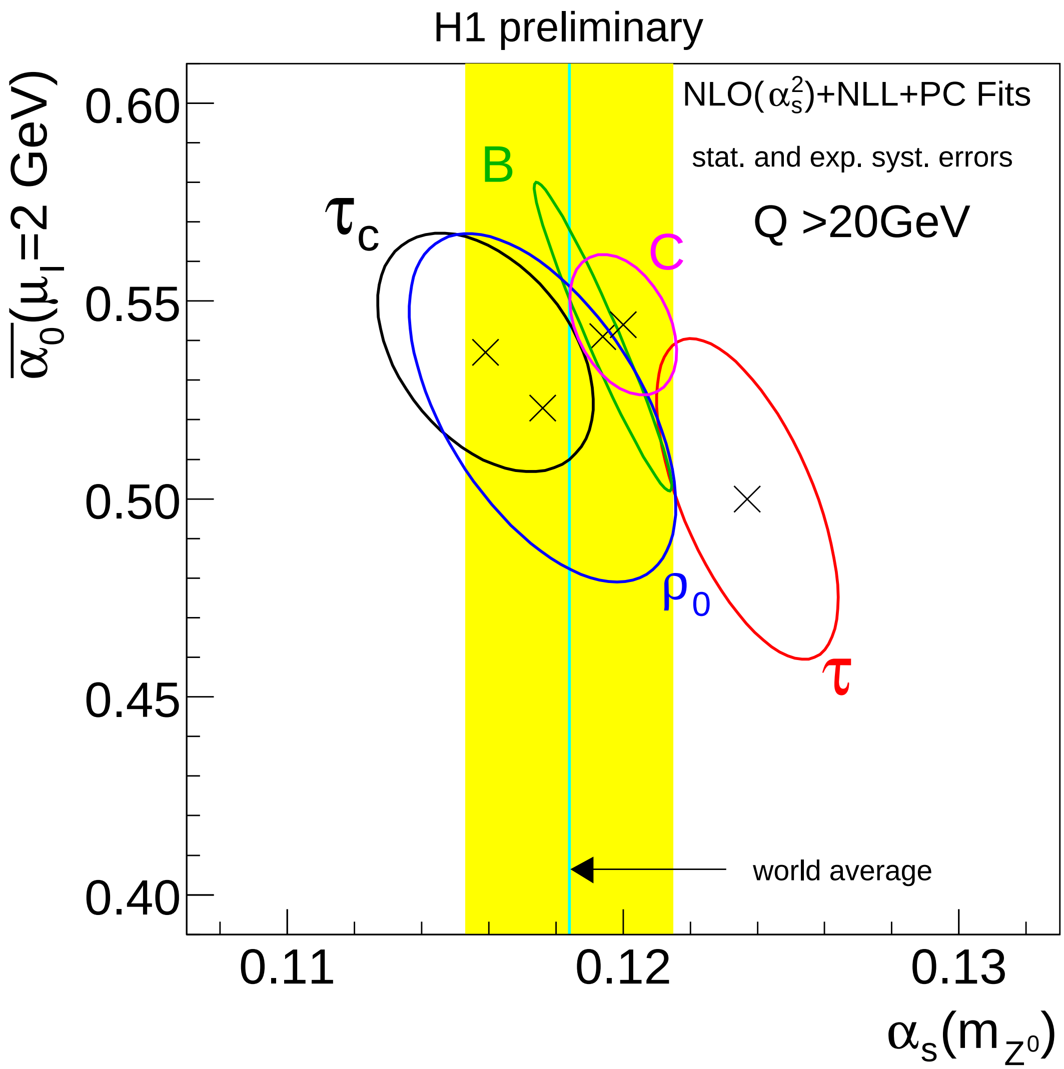

Figure 6: 1-σ contours in the (α_s, α_0) plane from fits to the 2 jet event shape differential distributions. The α_s band is taken from [12].

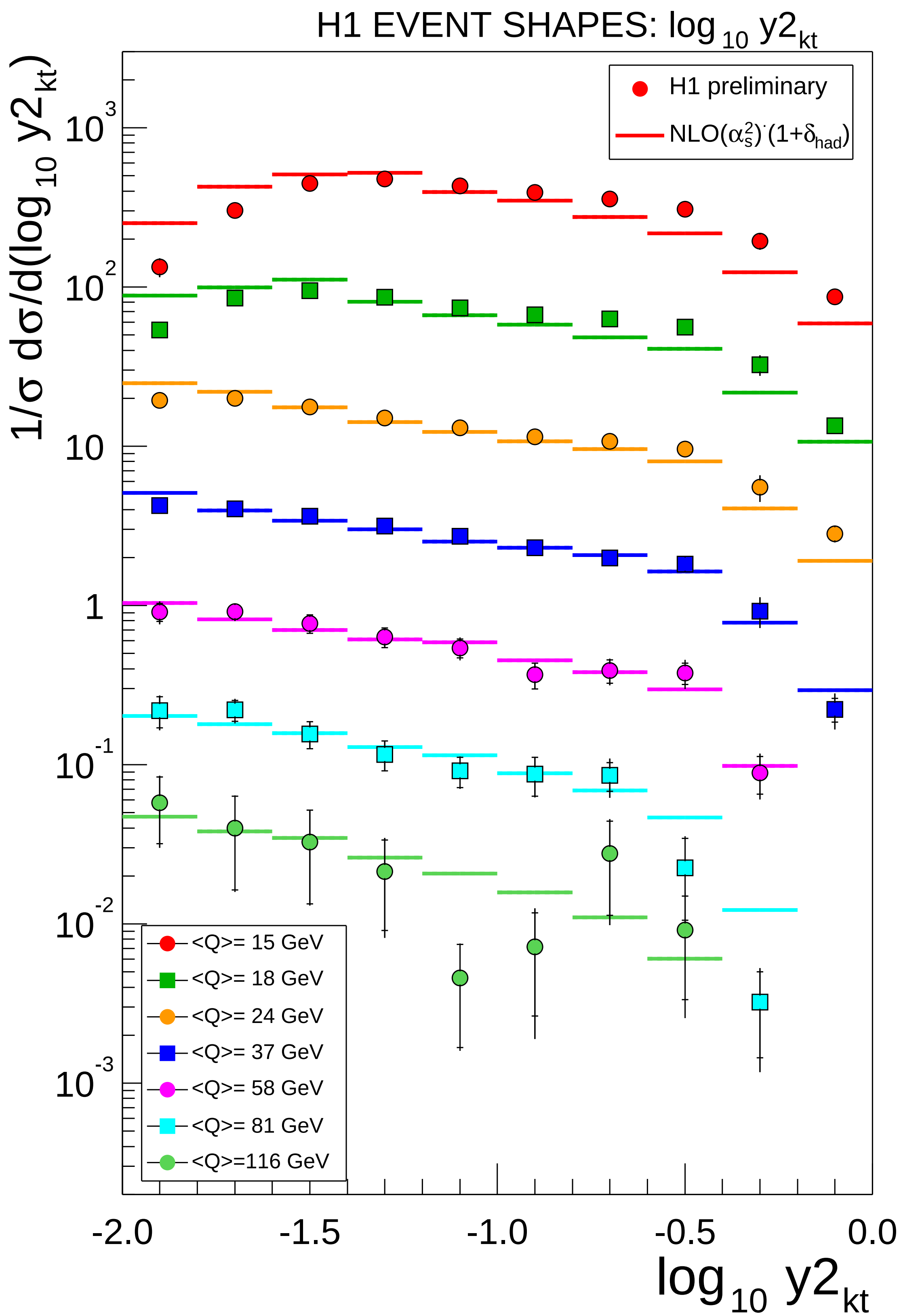

Figure 7: Measured values of the jet rate y_2, averaged over e^+ and e^- data. The data are compared to NLO QCD with hadronization corrections.

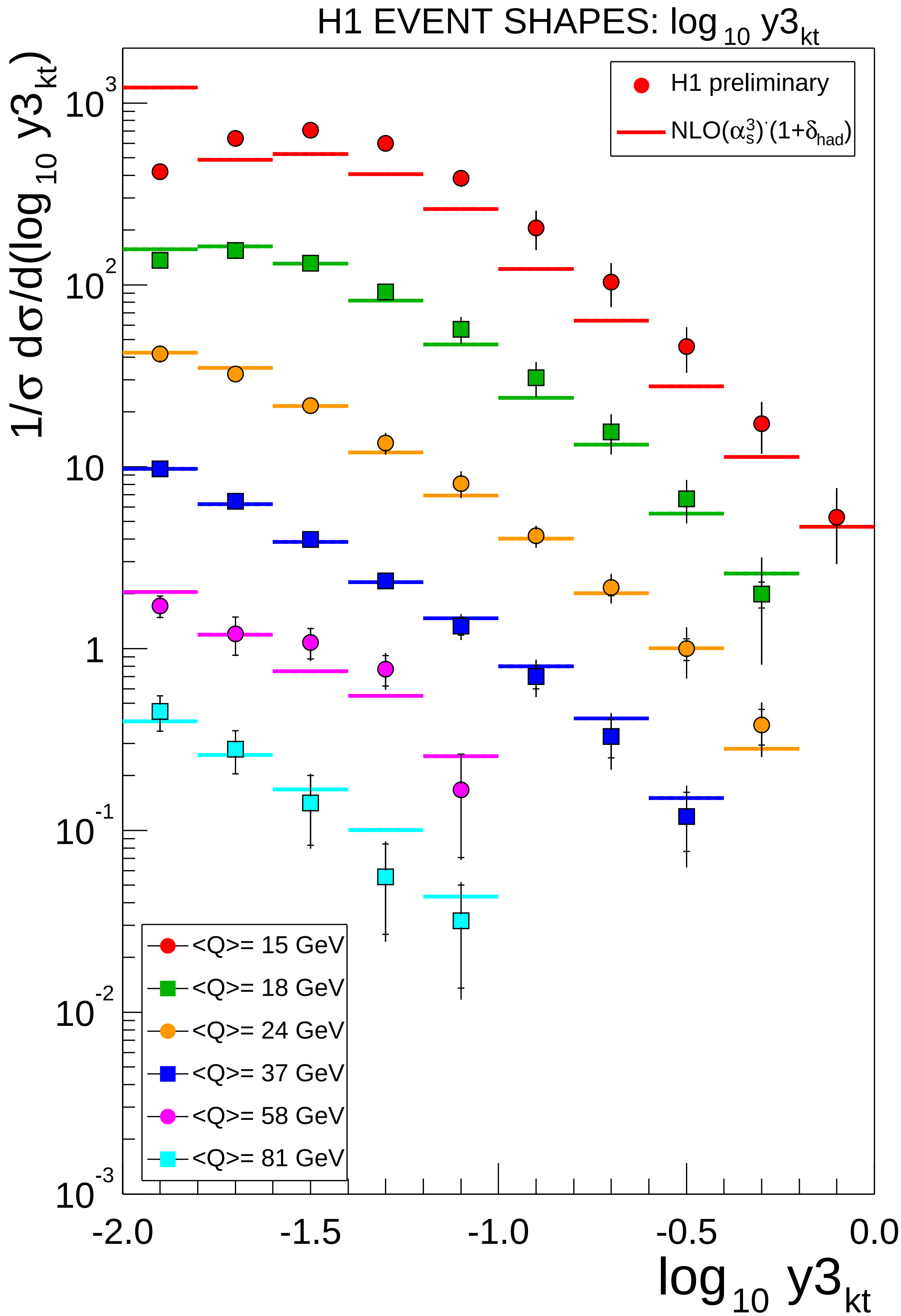

Figure 8: Measured values of the jet rate y_3, averaged over e^+ and e^- data. The data are compared to NLO QCD with hadronization corrections.

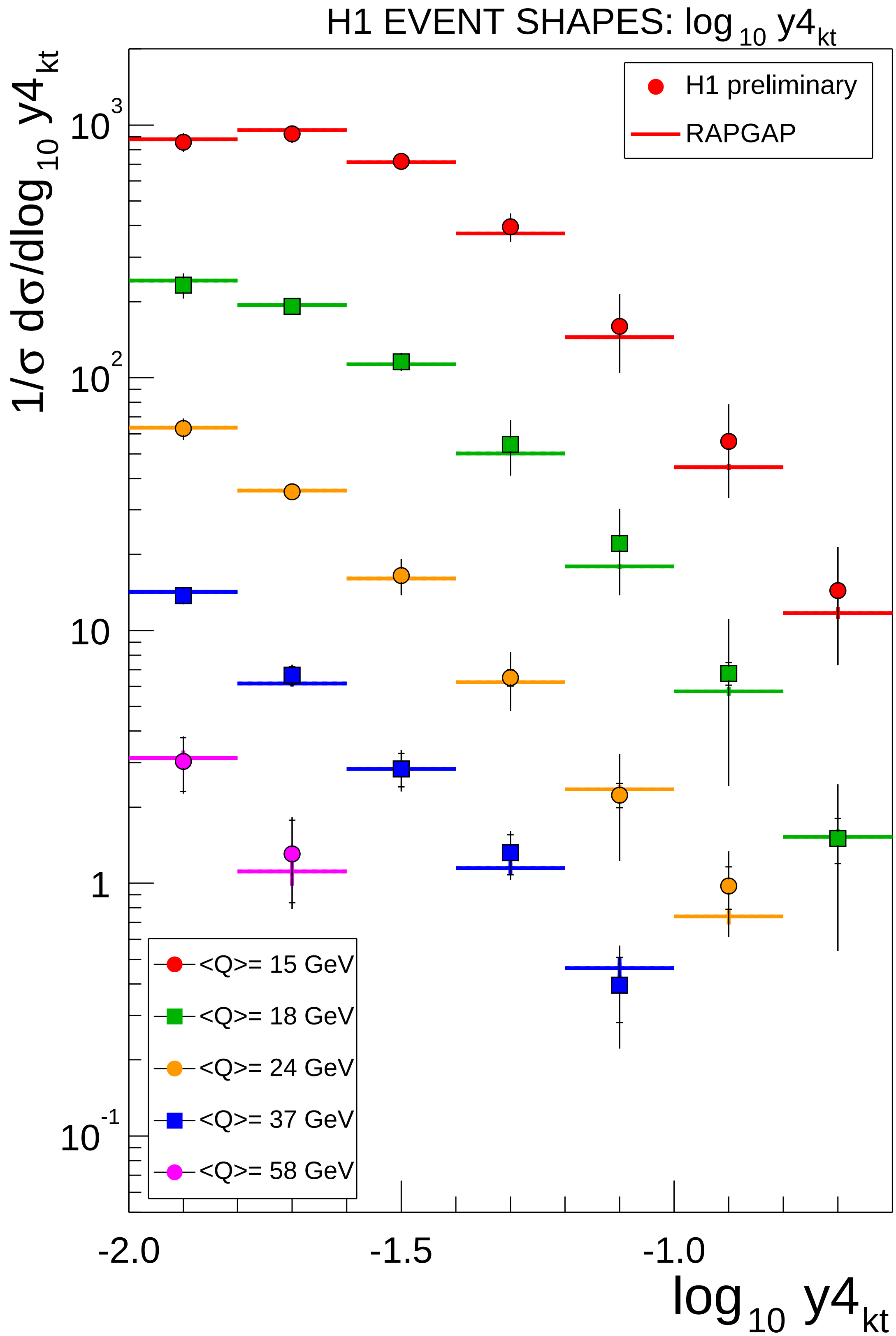

Figure 9: Measured values of the jet rate y_4, averaged over e^+ and e^- data. The data are compared with results from the RAPGAP Monte Carlo event generator.

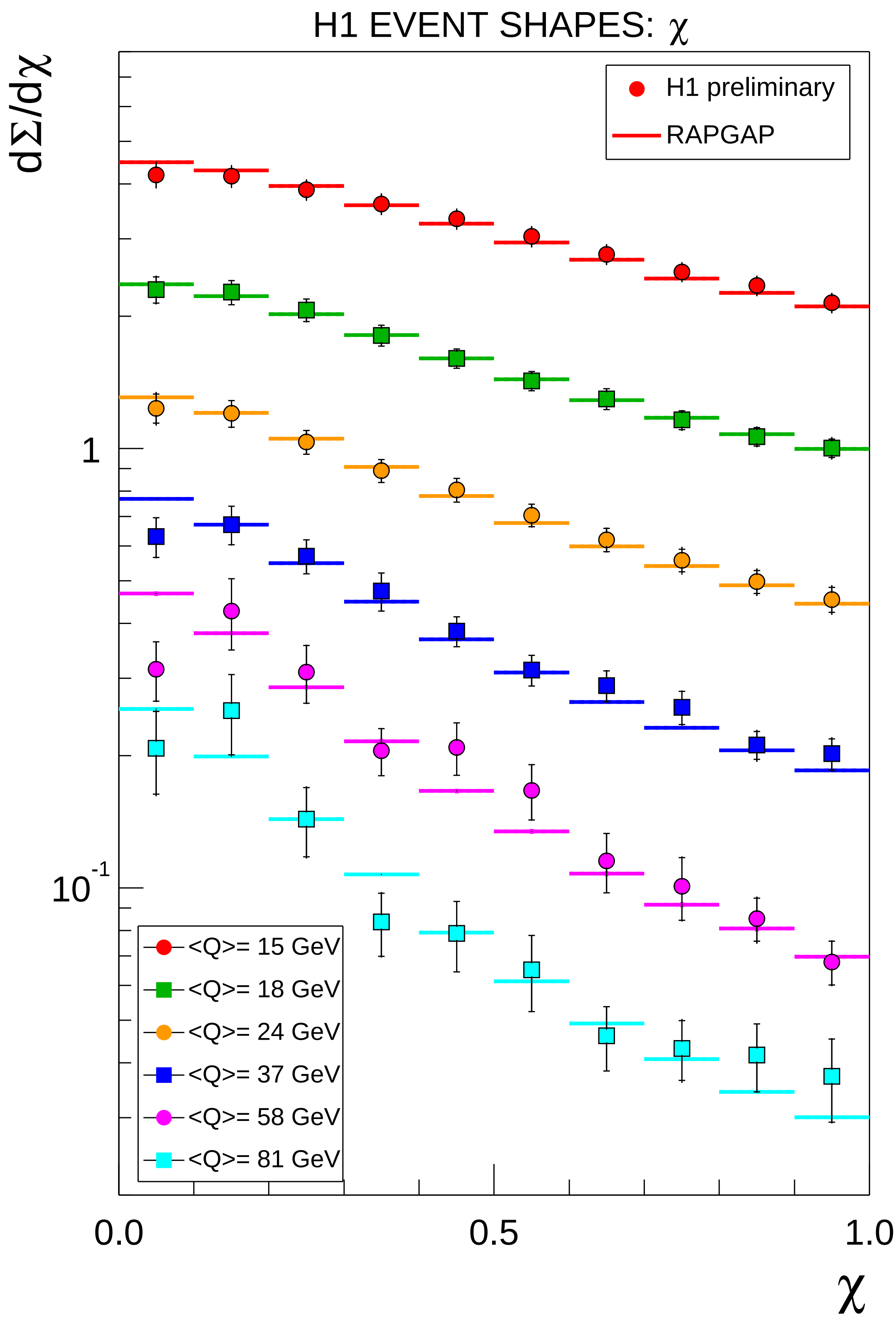

Figure 10: Measured values of azimuthal correlation χ, averaged over e^+ and e^- data. The data are compared with results from the RAPGAP Monte Carlo event generator.

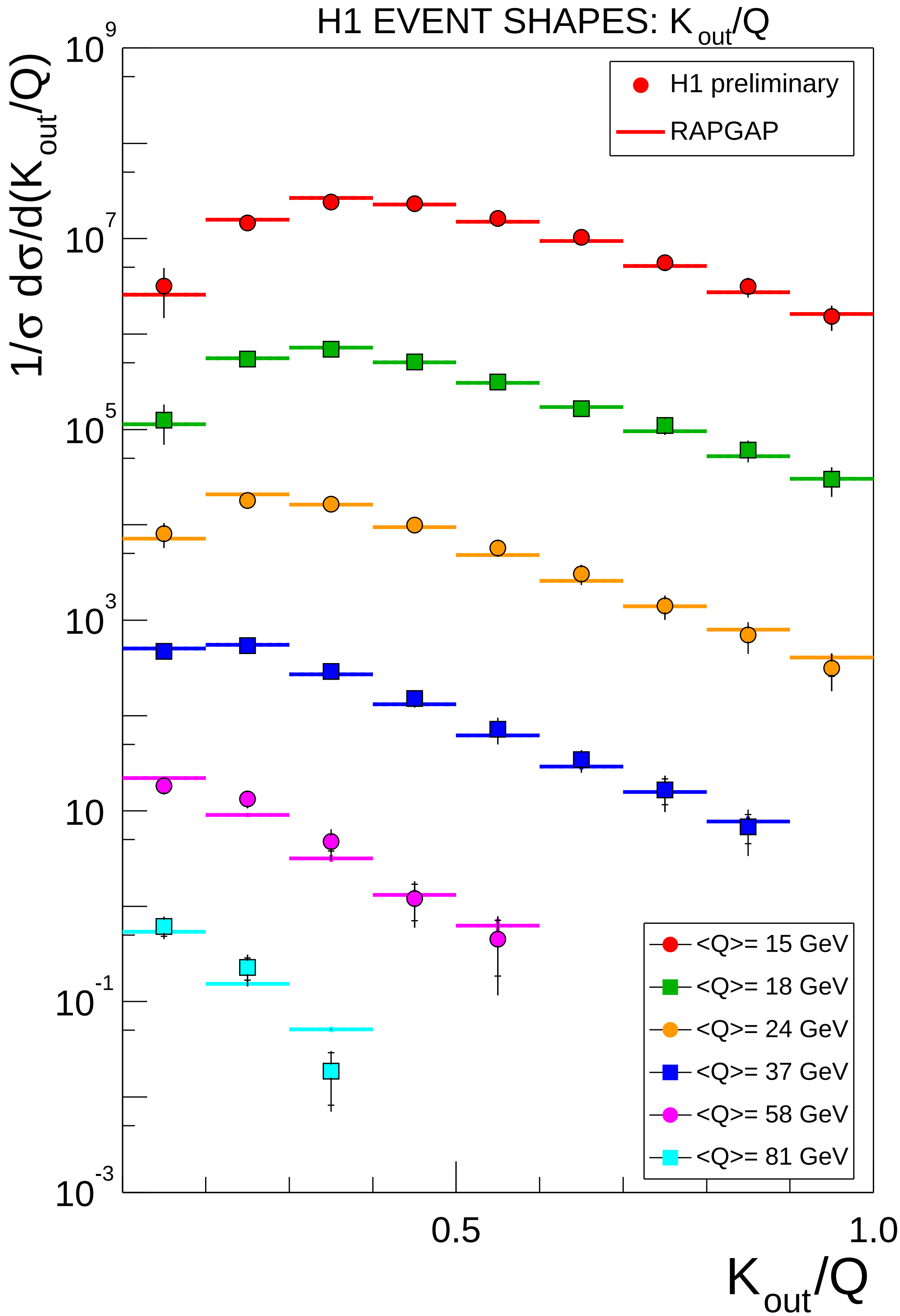

Figure 11: Measured values of out-of-plane momentum K_{out}, divided by Q and averaged over e^+ and e^- data. The data are compared with results from the RAPGAP Monte Carlo event generator.